Am J Transl Res 2019;11(7):4126-4138
www.ajtr.org /ISSN:1943-8141/AJTR0093756

Original Article

CircRNA LRP6 promotes the development of osteosarcoma *via* negatively regulating KLF2 and APC levels

Shengnai Zheng[1*], Zhanyang Qian[2*], Fan Jiang[2*], Dawei Ge[1], Jian Tang[2], Hongtao Chen[2], Jin Yang[3], Yilun Yao[1], Junwei Yan[1], Lei Zhao[1], Haijun Li[4], Lei Yang[1]

[1]Department of Orthopedic Surgery, Nanjing First Hospital, Nanjing Medical University, Nanjing 210006, Jiangsu, PR China; [2]Department of Orthopedics, The First Affiliated Hospital of Nanjing Medical University, Nanjing 210029, Jiangsu, PR China; [3]Department of Pathology, Wuxi Third People's Hospital, Wuxi 214000, Jiangsu, PR China; [4]Department of Orthopaedics, Taizhou People's Hospital Affiliated to Nantong University, Taizhou 225300, Jiangsu, PR China. [*]Equal contributors.

Received March 13, 2019; Accepted June 27, 2019; Epub July 15, 2019; Published July 30, 2019

Abstract: We aimed to investigate the biological functions of circLRP6 in the progression of osteosarcoma. CircLRP6 level in OS was detected by quantitative real-time polymerase chain reaction. Correlation between circLRP6 level with survival of OS patients was evaluated. Cell counting kit-8 and Transwell assay were conducted to detect proliferative, migratory and invasive capacities of OS cells. Cell cycle and apoptosis in OS cells influenced by circLRP6 were evaluated by flow cytometry. RNA immunoprecipitation was conducted to verify the binding relationship between circLRP6 with LSD1 and EZH2. Finally, the interaction between LSD1, EZH2 and promoter regions of KLF2, APC was clarified by chromatin immunoprecipitation. CircLRP6 level markedly increased in OS tissues. Besides, OS patients with high expression of circLRP6 showed shorter disease-free survival and over-all survival than those with low expression. CircLRP6 knockdown suppressed proliferative, migratory and invasive rates of OS cells. Moreover, circLRP6 knockdown induced apoptosis and arrested cell cycle in G0/G1 phase. The interaction between circLRP6 with LSD1 and EZH2 mediates their binding to the promoter regions of KLF2 and APC. Knockdown of circLRP6 weakened the binding abilities of LSD1, EZH2 to KLF2, APC. APC overexpression inhibited proliferation, induced apoptosis and arrested cell cycle. Moreover, the tumor-suppressor effect of downregulated circLRP6 on OS could be reversed by APC knockdown. Collectively, circLRP6 was highly expressed in OS and served as an oncogene by binding to LSD1 and EZH2 to inhibit expressions of KLF2 and APC.

Keywords: CircRNA LRP6, EZH2, LSD1, APC, osteosarcoma

Introduction

Osteosarcoma (OS) is a primary bone malignancy originating from osteoblasts. OS occurs at any age, but it mostly affects people with 10-25 years. The incidence of OS decreases with aging [1, 2]. Metaphysis of extremity long bones are frequently affected by OS, and lower femur and upper tibia in adolescents are the most typical affected bones [3]. Osteosarcoma cells are characterized by the formation of bone stroma, but their morphology obviously differs from that produced by osteoblasts. In recent years, researches on OS have focused on the biomacromolecules and gene levels. Studies have shown that the occurrence, development and metastasis of OS involve dysregulated biomolecules (i.e. activation of oncogenes and inactivation of tumor-suppressor genes), tumor microangiogenesis, imbalanced proliferation and apoptosis, and even gene mutations. These changes all contribute to the development of OS [4-6]. So far, the survival of OS patients is still unsatisfactory [7]. It is extremely important to search for effective diagnostic, therapeutic and prognostic hallmarks for OS.

CircRNA is a special class of non-coding RNAs. The special closed ring structure of circRNA allows it to be hardly degraded by RNA exonu-

clease, showing a much more stability [8-10]. Recent studies have confirmed the complex composition and multiple isoform types of circRNA, which is specifically expressed in various tissues. Functionally, circRNA exerts its biological function as a miRNA sponge to further mediate the downstream gene expressions. CircRNA-7 regulates mRNA levels of PARP and SP1 by absorbing miRNA-7a, which promotes cardiomyocyte death [11]. CircRNA-ITCH inhibits the expressions of miRNA-7, miRNA-17 and miRNA-214 in esophageal squamous cell carcinoma by sponge adsorption. Exogenous upregulation of circRNA-ITCH can inhibit the development of esophageal squamous cell carcinoma and the activation of the Wnt signaling pathway [12].

Previous studies have suggested that circLRP6 can upregulate ZEB1 expression and stimulate EMT process by adsorbing miR-455, thus improving cell migratory ability [13]. However, the role of circLRP6 in OS has not been reported. This study aims to elucidate the biological functions of circLRP6 in the development of OS at the cellular level.

Materials and methods

Subjects

OS tissues (n=50) and paracancerous normal bone tissues (n=50) were surgically resected from OS patients treated in Wuxi Third People's Hospital and The First Affiliated Hospital of Nanjing Medical University from September 2013 to December 2016. Tissues were pathologically diagnosed and immediately placed in liquid nitrogen. The enrolled OS patients did not have blood relationship between individuals. The experiment was approved by the Medical Ethics Committee of Wuxi Third People's Hospital and The First Affiliated Hospital of Nanjing Medical University. Informed consent of the patients was also obtained.

Cell culture and transfection

OS cell lines (Saos2, HOS, U2OS and MG63) and the normal human osteoblast cell line (hFOB1.19) were purchased from American Type Culture Collection (ATCC) (Manassas, VA, USA). Cells were cultured in the medium containing 10% fetal bovine serum (FBS) (Gibco, Rockville, MD, USA) and 1% penicillin/streptomycin, and preserved in a 37°C, 5% CO_2 incubator.

Before transfection, 2 mL of serum-free opti-MEM per well was added. Subsequently, circRNA mimics/siRNA/pcDNA and Lipofectamine™ 2000 (Invitrogen, Carlsbad, CA, USA) were diluted in reaction solution, respectively, and set at room temperature for 5 min. They were mixed together, set for another 20 minutes and supplied in each well. After incubation for 8 hours, antibiotics-free medium was replaced. Transfected cells were harvested at 48 hours.

RNA extraction and quantitative real-time polymerase chain reaction (qRT-PCR)

Total RNA was extracted using TRIzol (Invitrogen, Carlsbad, CA, USA), quantified and purified by UV spectrophotometer. 5 μg of total RNA was reversely transcribed into complementary deoxyribose nucleic acid (cDNA). QRT-PCR was performed using the Roche Light Cycler 480 Real-time PCR Amplifier under the following reactions: Pre-denaturation at 95°C for 2 min, amplification at 95°C for 15 s and annealing at 60°C for 1 min, for a total of 40 cycles. GAPDH was used as an internal reference. Relative levels of genes were calculated using the $2^{-\Delta\Delta Ct}$ method. Primer sequence were as follows: CircLRP6, F: CAAGATTGAGGCAGGCAGTG, R: GCTCCAGTCAGTCCAGTACA; GAPDH, F: GGGAGCCAAAAGGGTCAT, R: GAGTCCTTCCACGATACCAA; U1, F: GTAACCCGTTGAACCCCATT, R: CCATCCAATCGGTAGTAGCG; P21, F: AAGTCAGTTCCTTGTGGAGCC, R: GGTTCTGACGGACATCCCCA; KLF2, F: ACGGGCTTATTGAGGTTGG, R: GCCTGGGTGACAGAGGAGAC; APC, F: AGCCATGCCAACAAAGTCATCACG, R: TTCCTTGCCACAGGTGGAGGTA; BRCA1, F: GAAACCGTGCCAAAAGACTTC, R: CCAAGGTTAGAGAGTTGGACA; BRCA2, F: CACCCACCCTTAGTTCTACTGT, R: CCAATGTGGTCTTTGCAGCTAT.

Cell migration and invasion assays

50 mg/L Matrigel was diluted in high-glucose serum-free dulbecco's modified eagle medium (DMEM) (Gibco, Rockville, MD, USA) at a ratio of 1:8. 60 μL of diluted Matrigel was applied on the apical Transwell chamber. OS cells were prepared for suspension in high-glucose serum-free DMEM at 5×10^5 cells/mL. 100 μL of suspension and 700 μL of complete medium were

supplied on the basolateral and apical chamber, respectively, for 30-36 hours incubation. Subsequently, Transwell chamber was taken out and the medium was removed. Cell fixation using 4% paraformaldehyde and crystal violet dye were performed. Images were taken under a microscope for counting penetrating cells (magnification 20×). Procedures of cell migration assay were the same as the abovementioned except for Matrigel pre-coating.

Cell counting kit-8 (CCK-8) assay

Cells were digested to prepare the single cell suspension, and inoculated in a 96-well plate with 2×10^3 cells per well. At the appointed time points, fresh medium containing 10 μL of CCK-8 solution (Dojindo, Kumamoto, Japan) was replaced per well. After incubation for 2 hours, the recorded absorbance at 450 nm using a microplate reader was used for plotting the growth curve.

RNA immunoprecipitation (RIP)

Cells were collected and treated according to the procedures of Millipore Magna RIPTM RNA-Binding Protein Immunoprecipitation Kit (Billerica, MA, USA). Cell lysate was incubated with 5 μg of rabbit anti-human LSD1, EZH2 and CoREST, as well as rabbit IgG antibody at 4°C overnight. A protein-RNA complex was captured and digested with proteinase K to extract RNA fraction. The magnetic beads were repeatedly washed with RIP washing buffer to remove non-specific adsorption as much as possible. Finally, the extracted RNA was subjected to qRT-PCR.

Chromatin immunoprecipitation (ChIP)

Cells were cross-linked with 1% formaldehyde for 10 min at room temperature. Subsequently, the cross-linked cells were lysed using lysis buffer and sonicated for 30 min. Finally, the sonicated lysate was immuno-precipitated with antibodies and IgG.

Subcellular fractionation

1×10^6 cells were washed with pre-cold phosphate buffered saline (PBS), centrifuged and resuspended. Cell suspension was prepared for extracting the total RNA and cytoplasmic/nuclear RNA. The total RNA was extracted using TRIzol method. Cytoplasmic/nuclear RNA extraction was conducted using the PARISTM Kit Protein and RNA Isolation system (Thermo Fisher Scientific, Waltham, MA, USA). ΔCt value was calculated based on the formula: ΔCt = Relative nuclear level - Relative total level. The value of Lg ($2^{-\Delta Ct}$) was finally calculated. Lg ($2^{-\Delta Ct}$) > 0 indicated the target gene was mainly distributed in nucleus; Otherwise, it was mostly distributed in the cytoplasm.

Western blot

Total cellular protein was extracted using radioimmunoprecipitation assay (RIPA) (Beyotime, Shanghai, China) and denaturated at 100°C for 5 minutes. Protein sample was loaded for electrophoresis at 70 V for 30 minutes and 115 V for 65 minutes. After transferring on a polyvinylidene fluoride (PVDF) membrane (Millipore, Billerica, MA, USA) at 300 mA for 100 minutes, it was blocked in 5% skim milk for 2 hours, incubated with primary antibodies at 4°C overnight and secondary antibodies for 2 hours. Bands were exposed by electrochemiluminescence (ECL) and analyzed by Image Software.

Cell cycle determination

Cells were digested and fixed in pre-cold 70% ethanol at -20°C overnight. On the other day, cells were incubated with 10 μL of RNase for 30 minutes, dyed with propidium iodide (PI) for 15 minutes and finally subjected to flow cytometer determination.

Cell apoptosis determination

Cells were digested, resuspended in 200 μL of binding buffer and incubated with 10 μL of AnnexinV and 5 μL of PI for 15 minutes in dark. Finally, apoptosis was analyzed by a BD FACSCalibur flow cytometer (BD Bioscience, Franklin Lakes, NJ, USA) within 1 hour.

Statistical analyses

Statistical Product and Service Solutions (SPSS) 20.0 (IBM, Armonk, NY, USA) was used for all statistical analysis. Data were represented as mean ± SD. The *t*-test was used for analyzing difference between two groups, while those among multiple groups were analyzed by one-way ANOVA, followed by post-hoc test. Survival was evaluated by introducing for Kaplan-Meier method. Risk factors for survival were exam-

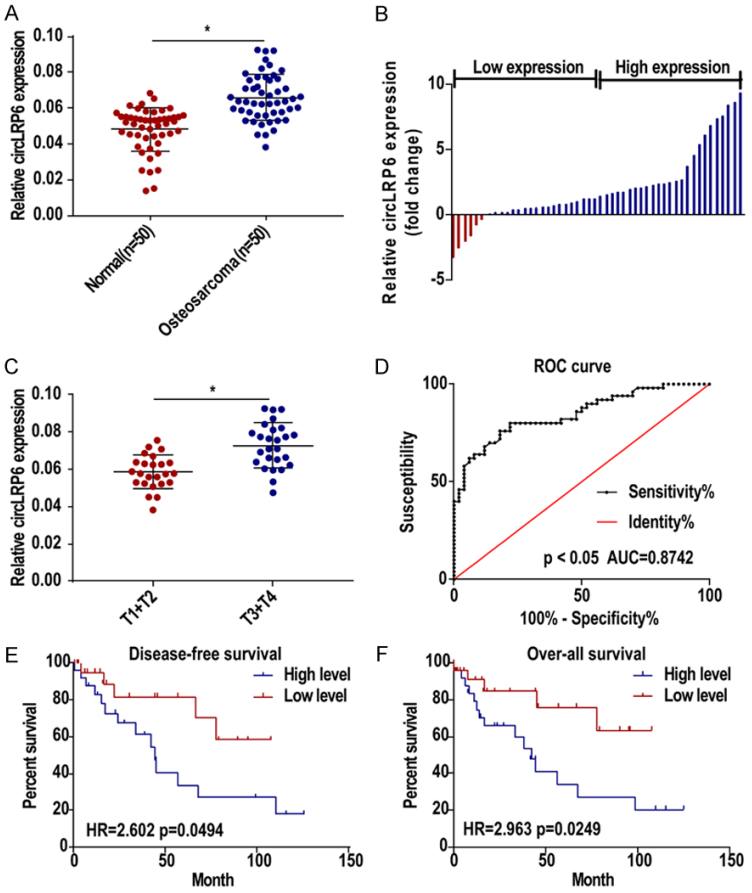

Figure 1. CircLRP6 expression remained high in OS. (A, B) CircLRP6 was highly expressed in OS tissues relative to normal ones (n=50). (C) CircLRP6 expression was higher in OS tissues with T1+T2 relative to those T3+T4 tissues. (D) ROC curve plotted based on circLRP6 expression in OS patients (AUC=0.8742). (E, F) OS patients with high level of circLRP6 showed shorter disease-free survival (E) and over-all survival (F) relative to those with low level. AUC, area under the curve; DFS, disease-free survival; OS: over-all survival. *P<0.05.

ined using Cox proportional hazards models. *P*<0.05 indicated the significant difference.

Results

CircLRP6 expression remained high in OS

First of all, circLRP6 expression in OS tissues (n=50) and paracancerous tissues (n=50) was determined by qRT-PCR. CircLRP6 was highly expressed in OS tissues relative to normal ones (**Figure 1A**, **1B**). Besides, circLRP6 expression remained higher in OS patients with T1+T2 relative to those with T3+T4 (**Figure 1C**). ROC curve was introduced to evaluate the potential of circLRP6 as a diagnostic marker for OS. The data confirmed the diagnostic potential of circLRP6, which was able to accurately distinguish OS tissues from normal ones (*P*<0.05, AUC= 0.8742, **Figure 1D**). Further, correlation between circLRP6 expression with disease-free survival and over-all survival was evaluated. It is found that OS patients with high level of circLRP6 showed shorter disease-free survival and over-all survival relative to those with low level (**Figure 1E**, **1F**). Univariate and multivariate analyses of prognosis revealed that circLRP6 expression, tumor size and lung metastasis were the independent risk factors for disease-free survival of OS patients (**Figure 2A**, **2B**). We also confirmed that the above three were the independent risk factors for over-all survival of OS patients as well (**Figure 2C**, **2D**). However, age, gender and tumor site of OS patients did not influence their prognosis. We may suggest the involvement of circLRP6 in the development of OS.

CircLRP6 regulated behaviors of OS cells

To investigate the biological function of circLRP6, we examined expression level of circLRP6 in osteoblasts (hFOB 1.19) and OS cell lines (Saos2, HOS, U2OS and MG63). CircLRP6 was highly expressed in HOS, U2OS and MG63 cells (**Figure 3A**). In particular, MG63 cells had a relatively high expression of circLRP6, while U2OS cells had a low expression, which were utilized for subsequent experiments. Transfection of si-circLRP6 in MG63 cells or pcDNA-circLRP6 in U2OS cells remarkably downregulated or upregulated circLRP6, respectively, proving their pronounced transfection efficacy (**Figure 3B**, **3C**). Knockdown of circLRP6 in MG63 cells decreased viability, induced apoptosis and arrested cell cycle progression in G0/G1 phase (**Figure 3D-F**). Conversely, overexpression of circLRP6 in U2OS cells increased viability, suppressed

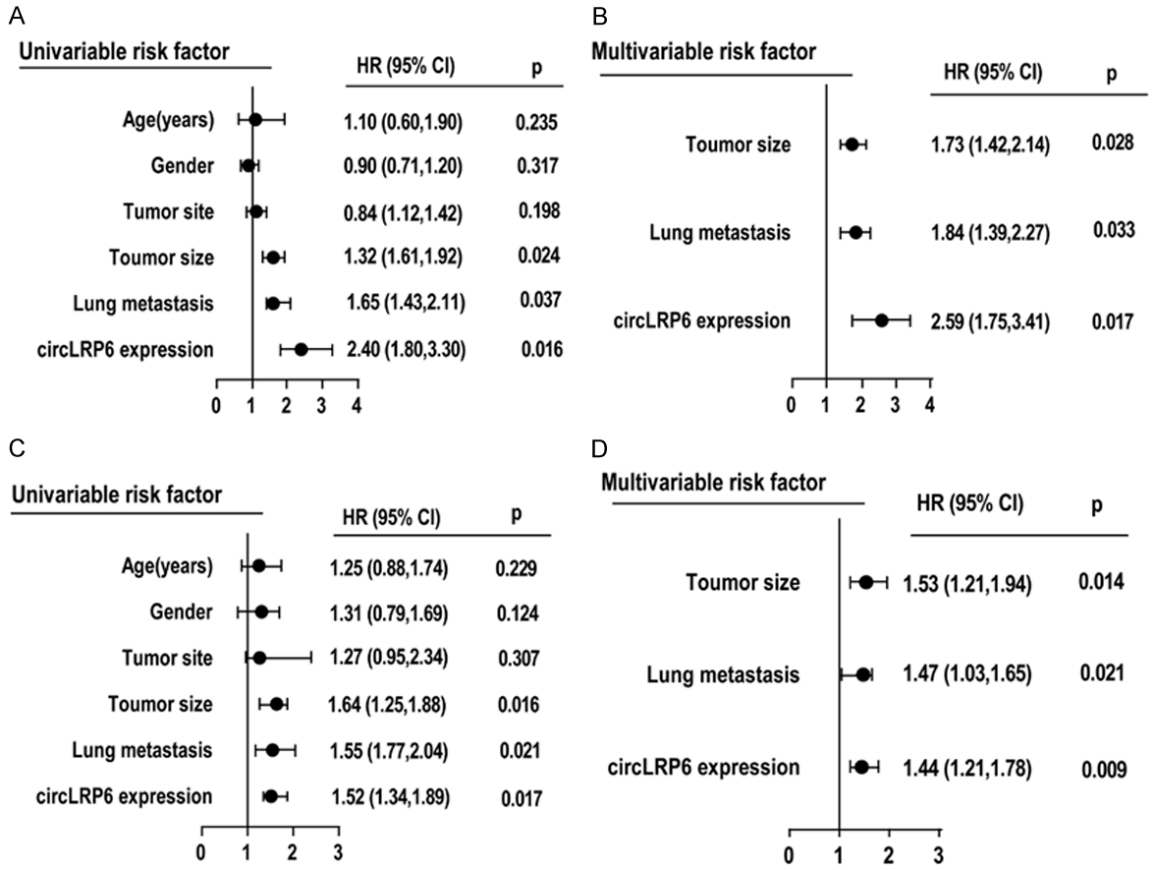

Figure 2. CircLRP6 was a risk factor for OS and DFS. A and B. Univariate analysis of Multivariate analysis of disease-free survival analysis in osteosarcoma patients showed that circLRP6 was an independent risk factors for disease-free survival. C and D. Univariate analysis of Multivariate analysis of over-all survival analysis in osteosarcoma patients showed that circLRP6 was an independent risk factors for over-all survival.

apoptosis and decreased cell ratio in G0/G1 phase (**Figure 3G-I**). Moreover, Transwell assay indicated that the migratory and invasive abilities of OS cells were positively regulated by circLRP6 (**Figure 3J**, **3K**).

CircLRP6 directly targeted on EZH2 and LSD1

Subcellular distribution of circLRP6 was explored here to further elucidate the potential mechanism. As qRT-PCR data revealed, circLRP6 was mainly distributed in the cytoplasmic fraction of U2OS and MG63 cells (**Figure 4A** and **4B**). Previous studies have shown that the tumor-regulatory functions of ncRNAs rely on RNA-binding proteins. Here, we examined the potential binding proteins with circLRP6 in U2OS and MG63 cells by RIP assay. It is shown that circLRP6 could bind to LSD1 and EZH2, while had no binding relationship with CoREST (**Figure 4C** and **4D**). Further, we hypothesized that abnormally expressed circLRP6 would affect downstream tumor-suppressor genes of LSD1 and EZH2. The mRNA levels of KLF2 and APC were upregulated, while p21, BRCA1 and BRCA2 levels did not alter after circLRP6 knockdown (**Figure 4E** and **4F**). Besides, expression level of circLRP6 was identified to be correlated with KLF2 and APC (**Figure 4G** and **4H**). Similar results were yielded at their protein levels (**Figure 4I**).

To confirm the regulatory effects of LSD1 and EZH2 on KLF2 and APC, we examined expression levels of KLF2 and APC in OS cells with LSD1/EZH2 knockdown. The mRNA levels of KLF2 and APC were markedly upregulated by transfection of si-LSD1 or si-EZH2 (**Figure 5A**). ChIP assay further verified the interaction between LSD1 and EZH2 with promoter regions of KLF2 and APC. Identically, histones H3K27me3 and H3K4me2 could bind to promoter regions

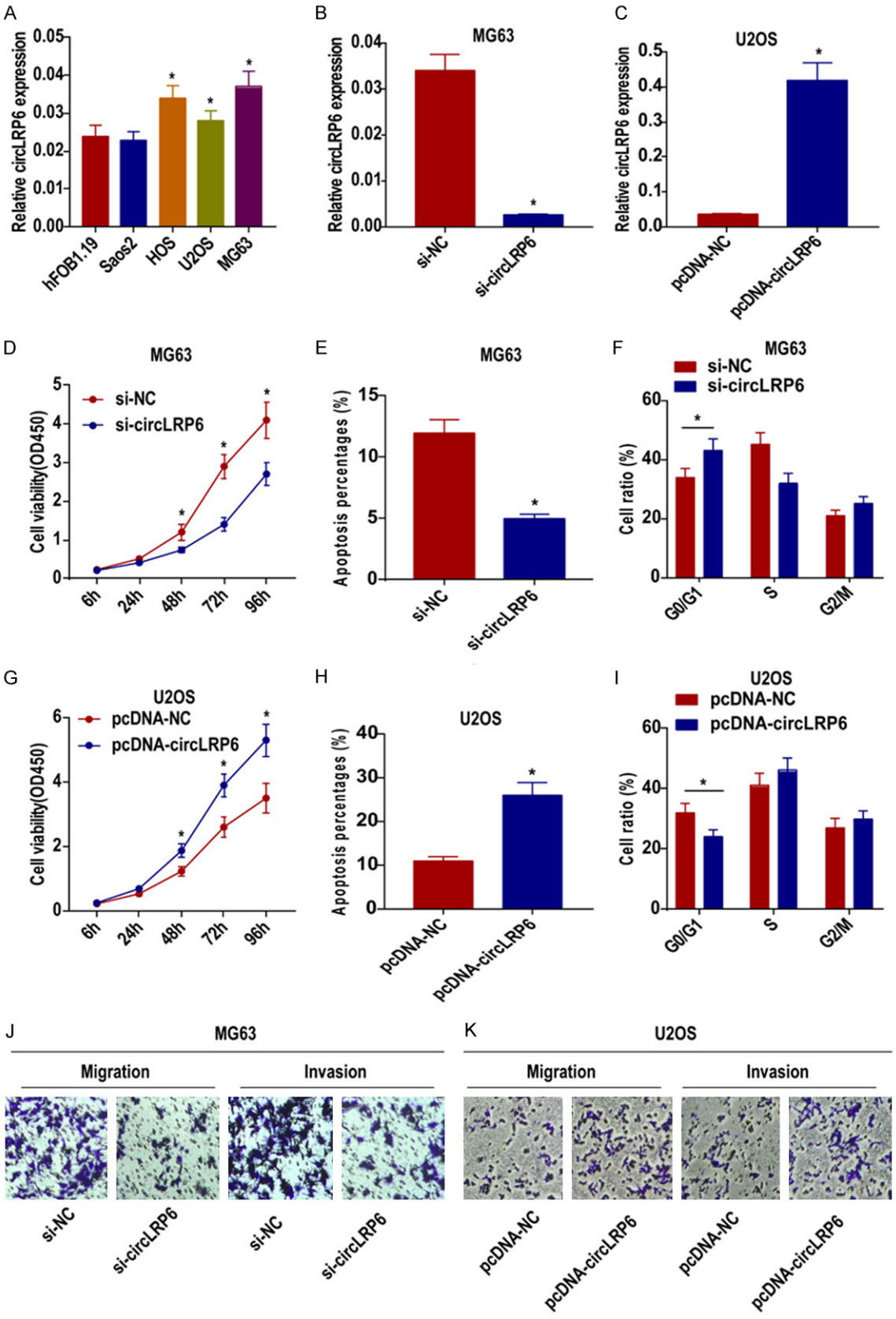

Figure 3. CircLRP6 regulate phenotype of osteosarcoma cells. A. Expression level of circLRP6 was highly expressed in U2OS and MG63 cells. B, C. Si-circLRP6 could downregulate circLRP6 in MG63 cells and pcDNA-circLRP6 could

up-regulate circLRP6 in U2OS cells. D. CCK-8 assay showed that knockdown of circLRP6 in MG63 cells decreased cell viability. E. Flow cytometry showed that knockdown of circLRP6 in MG63 cells induced apoptosis. F. Flow cytometry showed that knockdown of circLRP6 in MG63 cells arrested cell cycle progression in G0/G1 phase. G. CCK-8 assay showed that overexpression of circLRP6 in U2OS cells increased cell viability. H. Flow cytometry showed that overexpression of circLRP6 in U2OS cells suppressed apoptosis. I. Flow cytometry showed that overexpression of circLRP6 in U2OS cells decreased cell ratio in G0/G1 phase. J. Transwell assay indicated that knockdown of circLRP6 in MG63 cells inhibited the migratory and invasive abilities. K. Transwell assay indicated that overexpression of circLRP6 in U2OS cells accelerated the migratory and invasive abilities. *P<0.05.

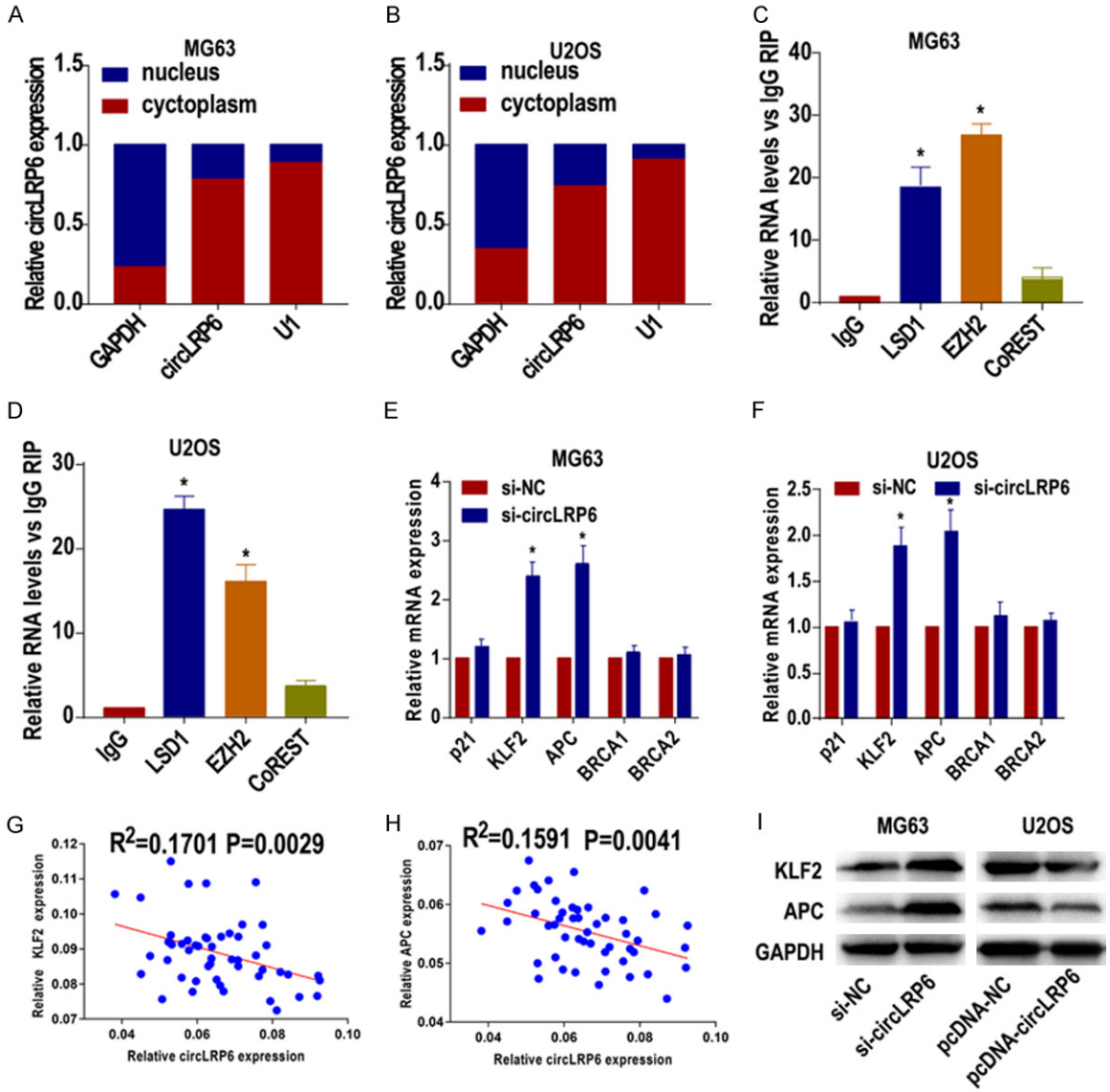

Figure 4. CircLRP6 directly bind to EZH2 and LSD1. A and B. QRT-PCR data revealed that circLRP6 was mainly distributed in the cytoplasmic fraction of U2OS and MG63 cells. GAPDH and U6 were served as cytoplasmic and nuclear internal references, respectively. C and D. RIP assay showed that circLRP6 could bind to LSD1 and EZH2 in U2OS and MG63 cells. E and F. QRT-PCR showed that the mRNA levels of KLF2 and APC upregulated, while p21, BRCA1 and BRCA2 did not alter after circLRP6 knockdown. G and H. CircLRP6 level was negatively correlated with those of KLF2 and APC. I. Western blot analyses showed that the protein levels of KLF2 and APC upregulated after circLRP6 knockdown. *P<0.05.

of KLF2 and APC as well (**Figure 5B**). After knockdown of circLRP6, binding abilities of EZH2, LSD1, H3K27me3 and H3K4me2 to circLRP6 greatly attenuated (**Figure 5C**, **5D**). These re-

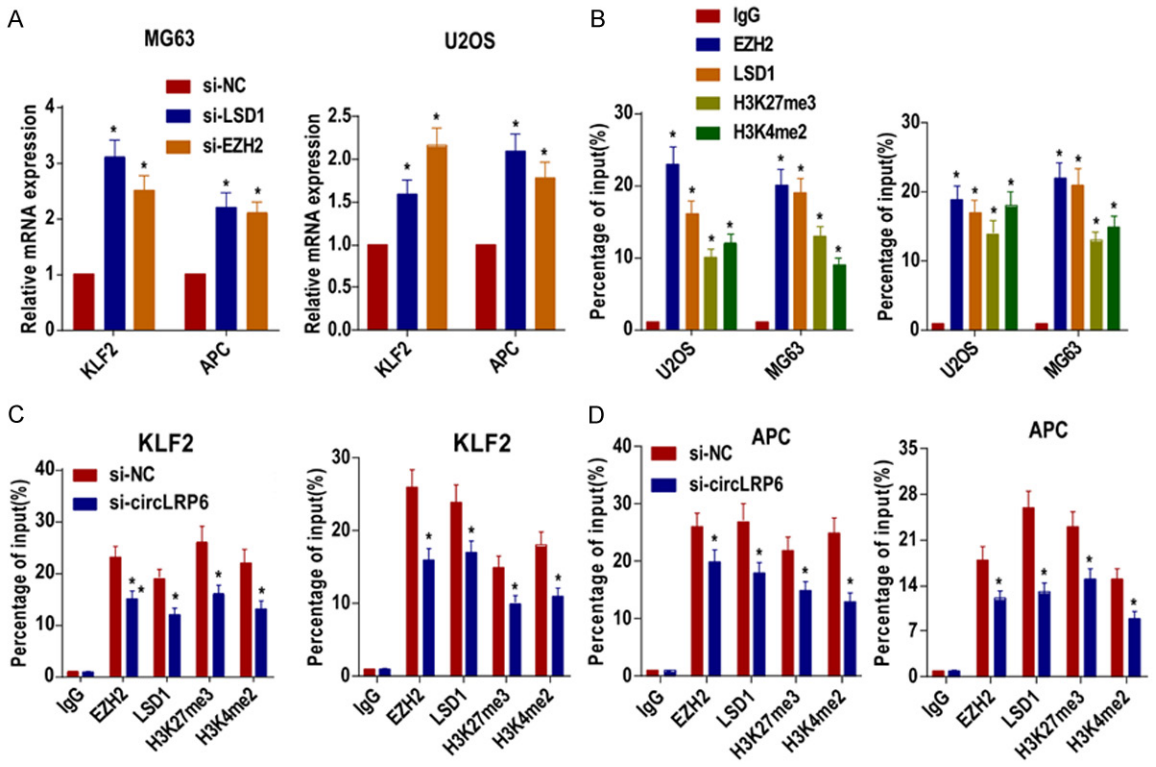

Figure 5. CircLRP6 inhibited expressions of KLF2 and APC by binding to EZH2 and LSD1. A. The mRNA levels of KLF2 and APC markedly upregulated by transfection of si-LSD1 or si-EZH2. B. ChIP assay verified the binding between LSD1, EZH2, H3K27me3 and H3K4me2 to the promoter regions of KLF2 and APC. IgG served as negative control. C, D. Knockdown of circLRP6 greatly attenuated binding abilities of EZH2, LSD1, H3K27me3 and H3K4me2 to circLRP6. *P<0.05.

sults suggested that circLRP6 bound to LSD1 and EZH2, and further regulated downstream tumor-suppressor genes.

CircLRP6 regulated the development of OS by mediating APC

To investigate the function of the target gene APC, transfection efficacy of pcDNA-APC in U2OS and MG63 cells was verified by Western blot (**Figure 6A**). CCK-8 assay showed reduced viabilities of U2OS and MG63 cells after overexpression of APC (**Figure 6B**). Meanwhile, APC overexpression arrested cell cycle in G0/G1 phase, and induced cell apoptosis (**Figure 6C**, **6D**). More importantly, APC knockdown could reverse the inhibited viability induced by circLRP6 knockdown in OS cells (**Figure 7A**). Transfection of si-APC also reversed the arrested cell cycle and increased apoptosis of OS cells with circLRP6 knockdown (**Figure 7B**, **7C**). Transwell assay indicated that the inhibitory effect of downregulated circLRP6 on migratory and invasive abilities of OS cells was reversed by APC knockdown (**Figure 7D**). These results suggested that circLRP6 exerted a tumor-promoting effect by inhibiting APC.

Discussion

In recent years, the specific function of circRNA in OS has been explored. CircRNA-NT5C2 is highly expressed in 52 pairs of OS tissues and OS cell lines. Functional experiments further confirmed that silence of circRNA-NT5C2 expression can inhibit the proliferative and invasive capacities, but induce apoptosis of OS cells [14]. Moreover, circRNA-UBAP2 is highly expressed in OS tissues, which accelerates OS growth and inhibits apoptosis of OS cells by absorbing miRNA-143 to enhance the activity of anti-apoptotic factor Bcl-2 [15]. In addition to the miRNA sponge function of circRNA, it may also regulate transcription and splicing at other levels, which requires for further explorations.

In this study, circLRP6 was highly expressed in OS tissues. As an independent risk factor for the prognosis of OS, patients with high expression of circLRP6 experienced shorter survival

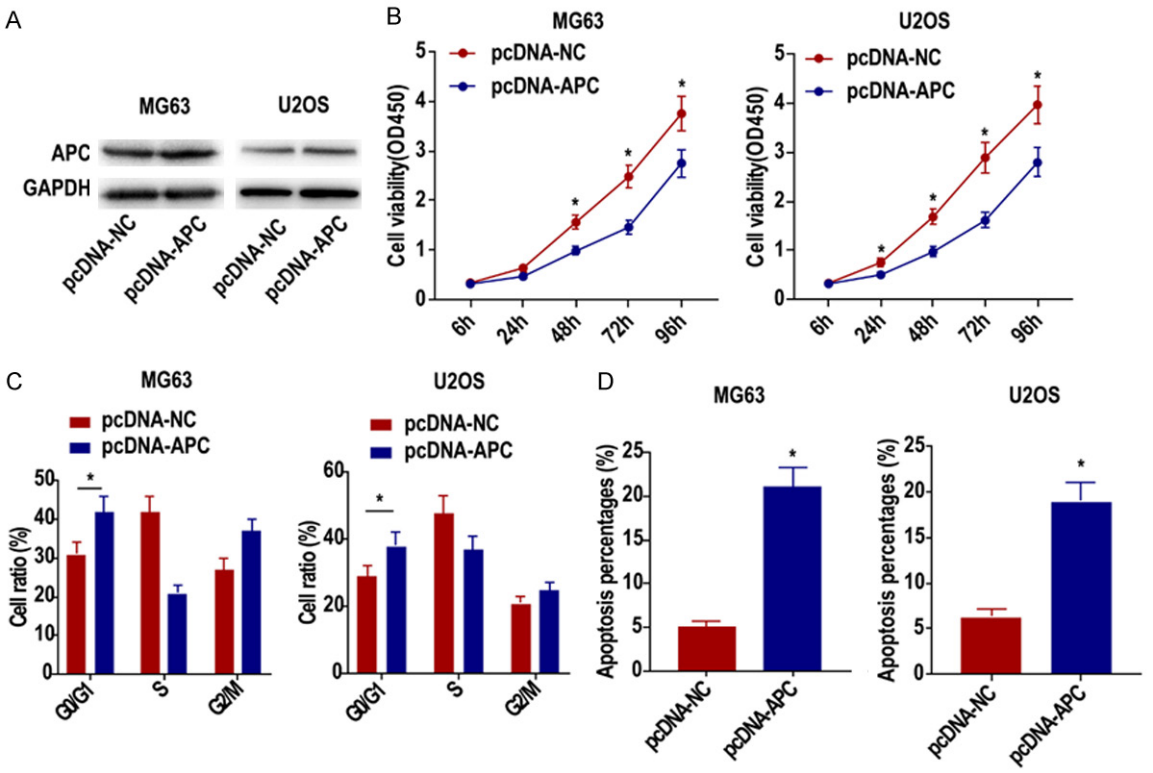

Figure 6. APC inhibited cell cycle progression and induced apoptosis of OS cells. A. The expression level of APC was up-regulated with transfection efficacy of pcDNA-APC in U2OS and MG63 cells verified by Western blot. B. CCK-8 assay showed reduced viability of U2OS and MG63 cells after overexpression of APC. C. APC overexpression arrested cell cycle of U2OS and MG63 cells in G0/G1 phase. D. APC overexpression induced apoptosis of U2OS and MG63 cells. *P<0.05.

than those with low expression. *In vitro* experiments revealed that circLRP6 knockdown inhibited proliferative, migratory and invasive capacities of OS cells. Moreover, knockdown of circLRP6 induced apoptosis, and arrested cell cycle progression in G0/G1 phase. Furthermore, circLRP6 was found to be mainly distributed in cytoplasm. We verified that circLRP6 was capable of regulating the binding of LSD1 and EZH2 to the promoter region of the target genes, thus mediating target gene expressions at transcriptional level (**Figure 8**).

LSD1 is a FAD-dependent amine oxidase distributed in the nucleus. It regulates gene expressions at transcriptional level, showing a crucial role in tumorigenesis and tumor progression [16]. In recent years, biological functions of LSD1 in tumors have been identified [17]. LSD1 regulates target gene expressions by specifically removing the methyl on the fourth lysine H3K4 and H3K9 of histone H3 [18]. However, biological functions of LSD1 vary a lot in different complexes [19]. For example, in a complex composed of LSD1/CoREST, BHC80, and HDAC1/2, LSD1 inhibits gene transcription by recognizing and demethylating H3K4-me1/2 [20]. It is reported that LSD1 expression increases with the aggravation of pathological grade, indicating its tumor-promoting effect. In colon cancer, LSD1 expression is related to E-cadherin, the EMT marker. LSD1 contributes to reduce the polarity, enhance the migratory and invasive abilities of colon cancer cells [21].

EZH2 inhibits apoptosis through a variety of signaling pathways and promotes proliferation by regulating oncogenes and tumor-suppressor genes at epigenetic level. RUNX3, a tumor-suppressor gene, is methylated by EZH2. The downregulated mRNA level of RUNX3, subsequently, promotes proliferative potential of tumor cells [22, 23]. EZH2 negatively regulates the epigenetics of DAB2IP promoter through silencing Ras expression, eventually accelerating growth and metastasis of prostate cancer

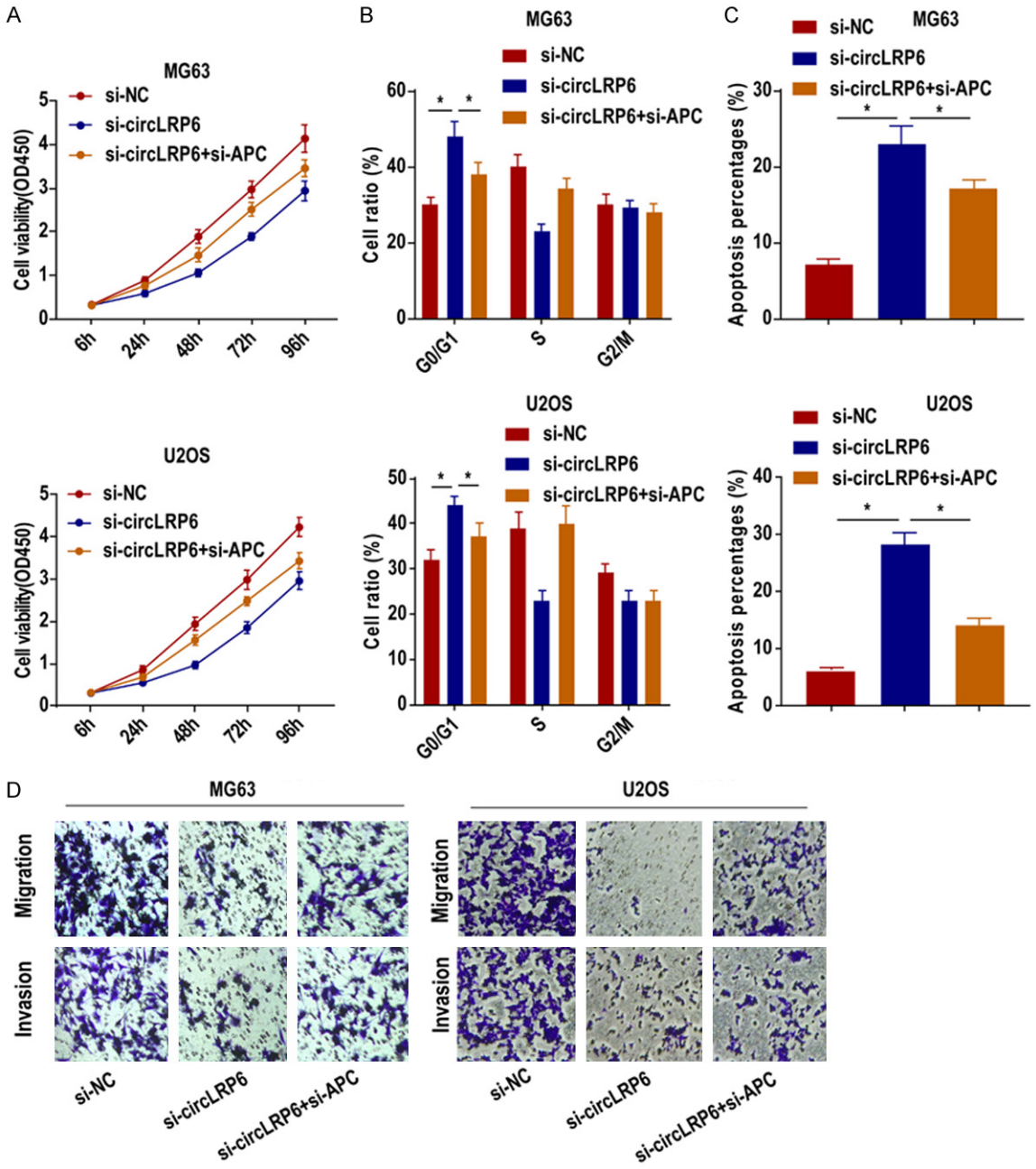

Figure 7. CircLRP6 regulated the development of OS by mediating APC. A. APC knockdown could reverse the inhibited viability induced by circLRP6 knockdown in U2OS and MG63 cells. B. Transfection of si-APC reversed the arrested cell cycle of U2OS and MG63 cells with circLRP6 knockdown. C. Transfection of si-APC reversed the increased apoptosis of U2OS and MG63 cells with circLRP6 knockdown. D. Transwell assay indicated that the inhibitory effect of circLRP6 knockdown on migratory and invasive abilities of U2OS and MG63 cells was reversed by APC knockdown. *P<0.05.

[24]. In undifferentiated thyroid cancer cells, EZH2 directly prevents proliferation inhibition and differentiation by silencing the thyroid-specific transcript PAX8 [25]. In addition, EZH2 also exerts a crucial role in tumor invasion and metastasis. EZH2 acts as an important inhibitory mediator to silence E-cadherin expression synergistically with histone deacetylase, thereby promoting migratory and invasive potentials of tumor cells [26]. In breast cancer cells, EZH2 can inhibit migratory and infiltrated abilities by suppressing the expression of FOXC1 [27].

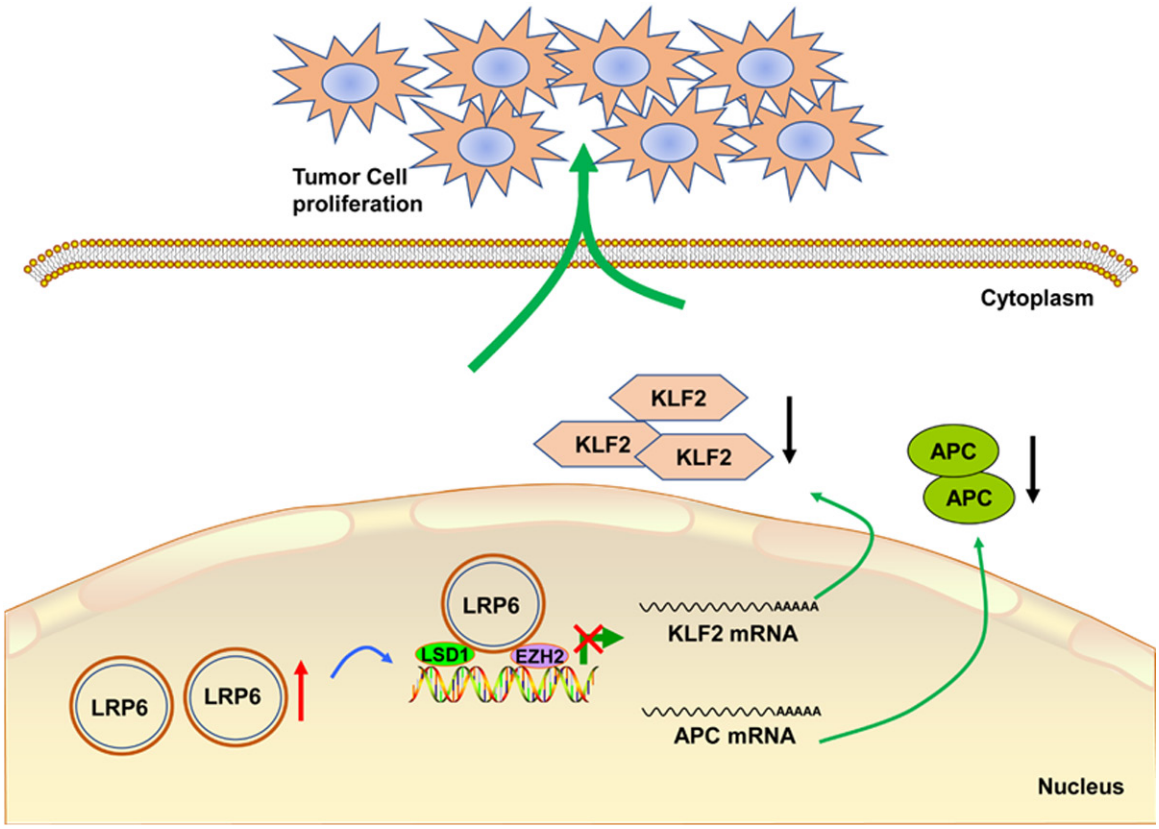

Figure 8. Proposed model in which circRNA LRP6 promotes progression of osteosarcoma.

EZH2 promotes migratory rates of breast and prostate cancer cells by transcriptionally inhibiting RKIP expression [28].

Our study found that knockdown of LSD1 and EZH2 resulted in the upregulation of tumor-suppressor genes KLF2 and APC. APC (adenomatous polyposis coli) locates at 5q21 and is an important tumor-suppressor gene in the Wnt pathway. It was first discovered in 1986 and has been widely investigated in tumor pathogenesis [29, 30]. Abnormal Wnt pathway caused by CpG methylation in the promoter region of APC gene is one of the crucial mechanisms responsible for tumorigenesis [31]. APC binds to and thus promotes the phosphorylation of β-catenin, and subsequently degrades it in the proteasome. APC deficiency impairs this process and leads to the cellular accumulation of β-catenin. Nuclear β-catenin further forms a complex with Tcf4, and finally results in uncontrolled cell growth. In addition to hyperproliferation, tumor cells are characterized with enhanced migratory and invasive capacities following the loss of epithelial features or the acquisition of interstitial features [32]. Studies have shown that APC knockdown allows accumulation of EMT biomarkers and activation of the Wnt pathway, which in turn affects cellular behaviors of tumor cells [33]. We believed that APC deficiency is one of the fundamental prerequisites for the EMT process. In this study, APC overexpression reversed the tumor inhibitory effect of downregulated circLRP6 on OS, indicating that circLRP6 promoted OS development by binding to LSD1 and EZH2 to inhibit APC expression.

However, there are still some shortcomings in this study. *In vitro* experiments conducted here at cellular level relied on the transient transfection method. Subsequent experiments should be carried out by lentivirus transfection. Besides, *in vivo* experiments are needed to elucidate the effects of circLRP6 on tumorigenesis and distant metastasis of OS.

Conclusions

CircLRP6 is highly expressed in OS and serves as an oncogene by binding to LSD1 and EZH2 to inhibit expressions of KLF2 and APC.

Acknowledgements

This study was supported by the National Natural Science Fund from the National Natural Science Foundation of China (Grant No. 818-02149) and Natural Science Foundation of Jiangsu Province (Grant No. BK20171089).

Disclosure of conflict of interest

None.

Address correspondence to: Dr. Lei Yang, Department of Orthopedic Surgery, Nanjing First Hospital, Nanjing Medical University, NO 68 Changle Road, Nanjing 210006, Jiangsu, PR China. E-mail: leiyang@njmu.edu.cn

References

[1] Geller DS and Gorlick R. Osteosarcoma: a review of diagnosis, management, and treatment strategies. Clin Adv Hematol Oncol 2010; 8: 705-718.

[2] Yang L, Ge D, Chen X, Qiu J, Yin Z, Zheng S and Jiang C. FOXP4-AS1 participates in the development and progression of osteosarcoma by downregulating LATS1 via binding to LSD1 and EZH2. Biochem Biophys Res Commun 2018; 502: 493-500.

[3] Ottaviani G and Jaffe N. The epidemiology of osteosarcoma. Cancer Treat Res 2009; 152: 3-13.

[4] Tian Z, Yang G, Jiang P, Zhang L, Wang J and Sun S. Long non-coding RNA Sox4 promotes proliferation and migration by activating Wnt/beta-catenin signaling pathway in osteosarcoma. Pharmazie 2017; 72: 537-542.

[5] Min X, Heng H, Yu HL, Dan M, Jie C, Zeng Y, Ning H, Liu ZG, Wang ZY and Lin W. Anticancer effects of 10-hydroxycamptothecin induce apoptosis of human osteosarcoma through activating caspase-3, p53 and cytochrome c pathways. Oncol Lett 2018; 15: 2459-2464.

[6] Lei Z, Duan H, Zhao T, Zhang Y, Li G, Meng J, Zhang S and Yan W. PARK2 inhibits osteosarcoma cell growth through the JAK2/STAT3/VEGF signaling pathway. Cell Death Dis 2018; 9: 375.

[7] Duong LM and Richardson LC. Descriptive epidemiology of malignant primary osteosarcoma using population-based registries, United States, 1999-2008. J Registry Manag 2013; 40: 59-64.

[8] Wilusz JE and Sharp PA. Molecular biology. A circuitous route to noncoding RNA. Science 2013; 340: 440-441.

[9] Jeck WR and Sharpless NE. Detecting and characterizing circular RNAs. Nat Biotechnol 2014; 32: 453-461.

[10] Zhang Y, Xue W, Li X, Zhang J, Chen S, Zhang JL, Yang L and Chen LL. The biogenesis of nascent circular RNAs. Cell Rep 2016; 15: 611-624.

[11] Geng HH, Li R, Su YM, Xiao J, Pan M, Cai XX and Ji XP. The circular RNA cdr1as promotes myocardial infarction by mediating the regulation of miR-7a on its target genes expression. PLoS One 2016; 11: e151753.

[12] Li F, Zhang L, Li W, Deng J, Zheng J, An M, Lu J and Zhou Y. Circular RNA ITCH has inhibitory effect on ESCC by suppressing the Wnt/beta-catenin pathway. Oncotarget 2015; 6: 6001-6013.

[13] Xue J, Chen C, Luo F, Pan X, Xu H, Yang P, Sun Q, Liu X, Lu L, Yang Q, Xiao T, Dai X, Luo P, Lu J, Zhang A and Liu Q. CircLRP6 regulation of ZEB1 via miR-455 is involved in the epithelial-mesenchymal transition during arsenite-induced malignant transformation of human keratinocytes. Toxicol Sci 2018; 162: 450-461.

[14] Liu X, Zhong Y, Li J and Shan A. Circular RNA circ-NT5C2 acts as an oncogene in osteosarcoma proliferation and metastasis through targeting miR-448. Oncotarget 2017; 8: 114829-114838.

[15] Zhang H, Wang G, Ding C, Liu P, Wang R, Ding W, Tong D, Wu D, Li C, Wei Q, Zhang X, Li D, Liu P, Cui H, Tang H and Ji F. Increased circular RNA UBAP2 acts as a sponge of miR-143 to promote osteosarcoma progression. Oncotarget 2017; 8: 61687-61697.

[16] Marabelli C, Marrocco B and Mattevi A. The growing structural and functional complexity of the LSD1/KDM1A histone demethylase. Curr Opin Struct Biol 2016; 41: 135-144.

[17] Lynch JT, Harris WJ and Somervaille TC. LSD1 inhibition: a therapeutic strategy in cancer? Expert Opin Ther Targets 2012; 16: 1239-1249.

[18] Fu X, Zhang P and Yu B. Advances toward LSD1 inhibitors for cancer therapy. Future Med Chem 2017; 9: 1227-1242.

[19] Forneris F, Binda C, Battaglioli E and Mattevi A. LSD1: oxidative chemistry for multifaceted functions in chromatin regulation. Trends Biochem Sci 2008; 33: 181-189.

[20] Kim J, Singh AK, Takata Y, Lin K, Shen J, Lu Y, Kerenyi MA, Orkin SH and Chen T. LSD1 is essential for oocyte meiotic progression by regulating CDC25B expression in mice. Nat Commun 2015; 6: 10116.

[21] Ding J, Zhang ZM, Xia Y, Liao GQ, Pan Y, Liu S, Zhang Y and Yan ZS. LSD1-mediated epigenetic modification contributes to proliferation and metastasis of colon cancer. Br J Cancer 2013; 109: 994-1003.

[22] Fujii S, Ito K, Ito Y and Ochiai A. Enhancer of zeste homologue 2 (EZH2) down-regulates RUNX3 by increasing histone H3 methylation. J Biol Chem 2008; 283: 17324-17332.

[23] Kodach LL, Jacobs RJ, Heijmans J, van Noesel CJ, Langers AM, Verspaget HW, Hommes DW, Offerhaus GJ, van den Brink GR and Hardwick JC. The role of EZH2 and DNA methylation in the silencing of the tumour suppressor RUNX3 in colorectal cancer. Carcinogenesis 2010; 31: 1567-1575.

[24] Beke L, Nuytten M, Van Eynde A, Beullens M and Bollen M. The gene encoding the prostatic tumor suppressor PSP94 is a target for repression by the Polycomb group protein EZH2. Oncogene 2007; 26: 4590-4595.

[25] Borbone E, Troncone G, Ferraro A, Jasencakova Z, Stojic L, Esposito F, Hornig N, Fusco A and Orlando V. Enhancer of zeste homolog 2 overexpression has a role in the development of anaplastic thyroid carcinomas. J Clin Endocrinol Metab 2011; 96: 1029-1038.

[26] Cao Q, Yu J, Dhanasekaran SM, Kim JH, Mani RS, Tomlins SA, Mehra R, Laxman B, Cao X, Yu J, Kleer CG, Varambally S and Chinnaiyan AM. Repression of E-cadherin by the polycomb group protein EZH2 in cancer. Oncogene 2008; 27: 7274-7284.

[27] Du J, Li L, Ou Z, Kong C, Zhang Y, Dong Z, Zhu S, Jiang H, Shao Z, Huang B and Lu J. FOXC1, a target of polycomb, inhibits metastasis of breast cancer cells. Breast Cancer Res Treat 2012; 131: 65-73.

[28] Ren G, Baritaki S, Marathe H, Feng J, Park S, Beach S, Bazeley PS, Beshir AB, Fenteany G, Mehra R, Daignault S, Al-Mulla F, Keller E, Bonavida B, de la Serna I and Yeung KC. Polycomb protein EZH2 regulates tumor invasion via the transcriptional repression of the metastasis suppressor RKIP in breast and prostate cancer. Cancer Res 2012; 72: 3091-3104.

[29] Wang Z, Tacchelly-Benites O, Yang E, Thorne CA, Nojima H, Lee E and Ahmed Y. Wnt/Wingless pathway activation is promoted by a critical threshold of axin maintained by the tumor suppressor APC and the ADP-ribose polymerase tankyrase. Genetics 2016; 203: 269-281.

[30] Blundon MA, Schlesinger DR, Parthasarathy A, Smith SL, Kolev HM, Vinson DA, Kunttas-Tatli E, McCartney BM and Minden JS. Proteomic analysis reveals APC-dependent post-translational modifications and identifies a novel regulator of beta-catenin. Development 2016; 143: 2629-2640.

[31] Liu S, Tackmann NR, Yang J and Zhang Y. Disruption of the RP-MDM2-p53 pathway accelerates APC loss-induced colorectal tumorigenesis. Oncogene 2017; 36: 1374-1383.

[32] Polyak K and Weinberg RA. Transitions between epithelial and mesenchymal states: acquisition of malignant and stem cell traits. Nat Rev Cancer 2009; 9: 265-273.

[33] Polakis P. Wnt signaling in cancer. Cold Spring Harb Perspect Biol 2012; 4: 1-10.